Seven-Hole Cone Probes for High Angle Flow Measurement: Theory and Calibration

K. N. Everett,* A. A. Gerner,* and D. A. Durston*
NASA Ames Research Center, Moffett Field, California

A non-nulling seven-hole conical pressure probe capable of measuring flow conditions at angles up to 75 deg relative to its axis is described. The theoretical rationale of the seven-hole probe is developed and the calibration procedure outlined. Three-variable third-order polynomial functions are used to represent local values of relative flow angles, total pressure, and total minus static pressure. These flow properties are determined explicitly from measured probe pressures. Flow angles are determined within 2.5 deg and Mach number within 0.05 with 95% certainty. The probe can be used in subsonic compressible and incompressible flows.

Nomenclature

A = any of four flow properties: α_T, β_T, Co, Cq for low angles and θ, ϕ, Co_n, Cq_n for high angles
C_M = compressibility effect coefficient
Co = total pressure coefficient
Cq = approximate dynamic pressure coefficient
C_α = intermediate angle coefficient
C_{α_T} = angle of attack coefficient: low angles
C_{β_T} = angle of sideslip coefficient: low angles
C_θ = pitch angle coefficient: high angles
C_ϕ = roll angle coefficient: high angles
K = calibration constant
M = Mach number
m = total number of data points in a given sector
P = probe port pressure
P_o = total pressure
P_∞ = static pressure
V = velocity
α = angle of attack
α_T = angle of attack, tangential reference system
β = angle of sideslip
β_T = angle of sideslip, tangential reference system
θ = pitch angle, polar reference system
ϕ = roll angle, polar reference system
σ = standard error

Subscripts

i = ith data point in a given sector
L = local property at probe tip
n = port or sector number (1-7)
n^+ = adjacent port clockwise to port n
n^- = adjacent port counterclockwise to port n

Introduction

AIRCRAFT designs that incorporate lift-enhancement devices, such as canards and leading-edge extensions (LEXs), are under study in several programs at the NASA Ames Research Center.[1] These lift-enhancement devices induce strong vortices with local flow angles often exceeding 60 deg relative to the freestream. An important aspect of these aircraft aerodynamic studies is visualization of the flow and measurement of the properties in these complex flows.

Aside from sophisticated theoretical methods, many flow visualization techniques serve only to locate flow regions of interest. Obtaining quantitative data often requires direct measurement of the flow. One of the oldest methods of direct flow measurement is the insertion of a probe into the flow. Two probes commonly used are the five-hole pressure probe and the triaxial hot-wire probe. Unfortunately, these probes are not accurate when the local flow angle exceeds 40 deg. Until now, obtaining data at higher flow angles required elaborate methods such as nulling probes or laser Doppler velocimetry.

This paper describes the theory and calibration of a non-nulling seven-hole conical pressure probe capable of rapidly providing quantitative flow data through high angles of attack. The probe is the product of a joint research effort between NASA Ames and the U.S. Air Force Academy to measure and study canard wakes.

In order to minimize flow disturbance, the probes are made very small (about 0.25 cm in diameter). However, due to their small size, unavoidable manufacturing irregularities require that each probe be calibrated. Calibration establishes polynomial expressions which are used to calculate local flow properties during a flow survey.

Previous probe calibrations, similar to those described herein, have been conducted at the U.S. Air Force Academy. The first two calibrations were conducted at single, very low, Mach numbers (incompressible flow).[2] A subsequent calibration encompassed both compressible and incompressible flows, covering a Mach number range of 0.37-0.91 (Ref. 3). However, due to time and hardware constraints, only a limited amount of data was taken. As a result, the data matrix of this latter test was selected using the method of Latin Squares. Although the method of Latin Squares is a feasible approach for calibration, data obtained using this technique are not well adapted to the study of the flow conditions and probe pressure relationships.

The probe calibration performed at the NASA Ames Research Center covered both compressible and incompressible flows, due to greater tunnel time and hardware flexibilities, a much larger data set was taken. The NASA Ames calibration also investigated Reynolds number effects, which were not examined previously.

This paper outlines the calibration theory and procedure and describes the calibration of four seven-hole probes in the Ames 2×2-ft transonic wind tunnel. The results of the calibration are discussed and analyzed and the capabilities of the probe are summarized.

Calibration Theory

The calibration theory develops equations from which the desired flow properties are determined explicitly. Gallington[2]

Presented as Paper 82-0232 at the AIAA 20th Aerospace Sciences Meeting, Orlando, Fla., Jan. 11-14, 1982; submitted Jan. 22, 1982; revision received Oct. 8, 1982.

*Aerospace Engineer. Member AIAA.

describes such a procedure using polynomial functions in two angular variables. However, this technique neglects compressibility effects. Inclusion of a variable representative of compressibility effects allows the calibration to be extended into the compressible flow regime.[3] The three variables are expressed as dimensionless pressure coefficients, in terms of probe-measured pressures.

Low Angles

The tangential system (Fig. 1) is adopted for low flow angles (angles typically less than 25 deg). The term α_T is the angle between the probe's x axis and the projection of the velocity vector on the vertical plane. The term β_T is defined as the angle between the probe's x axis and the projection of the velocity vector on the horizontal plane. This system is similar to the more familiar α-β reference system, differing only in the definition of the sideslip angle.

At low angles, the flow over all seven pressure ports is attached. Hence, all seven pressures are used to define the angular pressure coefficients which vary nearly linearly with changes in flow angularity. From Fig. 2, a pressure coefficient sensitive to changes in angle of attack may be defined as

$$C_\alpha = (P_4 - P_1)/(P_7 - \bar{P}_{1\text{-}6}) \tag{1}$$

where the numerator measures changes in the angle of attack based on the difference in opposite port pressures, and the denominator nondimensionalizes the term with the probe dynamic pressure. This probe dynamic pressure is obtained from the difference between the center port pressure P_7, which (at low angles) approximates the total pressure, and the average of the six surrounding pressures $\bar{P}_{1\text{-}6}$, which approximates the static pressure.

Strictly speaking, the difference between the total and static pressures is the dynamic pressure only for incompressible flow. However, throughout this discussion, the *approximate dynamic pressure* refers to the difference between the total and static pressures, which is not necessarily the true dynamic pressure. Similarly, the *probe dynamic pressure* refers to the difference between the probe's closest approximation to the total and static pressures.

Due to symmetry, two other pressure coefficients can be defined which use 1) the differential between ports three and six, and 2) the differential between ports two and five. To differentiate among these coefficients, the coefficient in Eq. (1) is designated $C_{\alpha a}$ and the two remaining coefficients are designated $C_{\alpha b}$ and $C_{\alpha c}$, respectively. The complete set of these pressure coefficients is

$$C_{\alpha_a} = \frac{P_4 - P_1}{P_7 - \bar{P}_{1\text{-}6}}, \quad C_{\alpha_b} = \frac{P_3 - P_6}{P_7 - \bar{P}_{1\text{-}6}}, \quad C_{\alpha_c} = \frac{P_2 - P_5}{P_7 - \bar{P}_{1\text{-}6}} \tag{2}$$

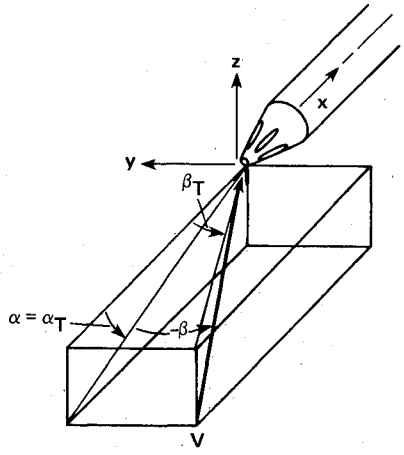

Fig. 1 Low angle reference system.

These coefficients correspond to the reference system depicted in Fig. 2a. Only two of the three coefficients are needed to uniquely specify the orientation of an oncoming velocity vector. As a result, three equally valid solutions exist, depending on which pair of coefficients is selected.

To arbitrarily select a pair of coefficients eliminates the additional pressure information available in the third coefficient. To avoid this loss of information, equal weightings of the three solutions from the C_{α_a}-C_{α_b}-C_{α_c} reference system are resolved into a single ordered pair, C_{α_T} and C_{β_T} in the tangential reference system (Fig. 2b). This transformation is outlined in Ref. 2 and results in the following equations:

$$C_{\alpha_T} = \frac{1}{3}(2C_{\alpha_a} + C_{\alpha_b} - C_{\alpha_c}), \quad C_{\beta_T} = \frac{1}{\sqrt{3}}(C_{\alpha_b} + C_{\alpha_c}) \tag{3}$$

Equations (3) constitute two of the three coefficient variables used in the polynomial functions. The remaining variable is a coefficient of compressibility effects (denoted C_{M_n}). Two requirements are imposed on this coefficient: 1) it must approach zero as the Mach number approaches zero, and 2) it must approach a finite value in the hypersonic limit. These requirements are satisfied by modeling the compressibility coefficient after the approximate dynamic to total pressure ratio vs Mach number relationship for isentropic flow. A compressibility relationship of this form is valid throughout the subsonic regime. Using the probe's approximation for dynamic and total pressure at low flow angles, the compressibility coefficient is given by

$$C_{M_7} = (P_7 - \bar{P}_{1\text{-}6})/P_7 \tag{4}$$

High Angles

A reference system better suited to high flow angle measurements is the polar system (Fig. 3). The pitch angle θ measures the total angle between the velocity vector and the probe's x axis. The roll angle ϕ is the azimuthal angle between the negative z axis and the projection of the velocity vector in the y-z plane. The angle ϕ is measured positive from the negative z axis in a counterclockwise direction as viewed from the front.

Unlike flow at low angles, flow at high angles tends to separate over the downstream portion of the probe (Fig. 4). Typically, for turbulent flow, the separation points of flow around a circular cylinder are over 100 deg from the upstream stagnation point.[4] Since the probe tip is a conical surface and receives a forward velocity component, the actual separation points are likely to extend beyond those of a cylinder.[4] Figure 4 depicts such a high angle flow condition for a roll angle of 0 deg, where the velocity vector is directed at port four. Pressure ports three, four, five, and seven are in attached flow. Pressure port one lies in the separated wake, and the flow condition over ports two and six is uncertain.

Pressure ports lying within the separated region are insensitive to changes in stream angularity. As a result, the coefficients must be defined based on pressures from ports

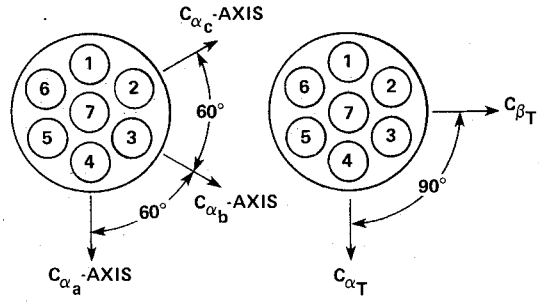

Fig. 2 Angular coefficient reference systems, a) three coefficient axis system and b) tangential reference system.

lying in reliably attached flow. This is ensured by confining the coefficients defined for the situation in Fig. 4 to roughly a 60-deg pie-shaped sector centered on port four. To handle the remaining possible flow directions, five additional sets of coefficients are defined. Each set is confined to roughly a 60-deg sector centered on one of the remaining periphery pressure ports.

Using ports lying in reliably attached flow for the situation in Fig. 4, a coefficient sensitive to changes in pitch angle takes on the form

$$C_{\theta_4} = \frac{P_4 - P_7}{P_4 - (P_3 + P_5)/2} \tag{5}$$

This equation uses a rationale similar to that used in developing Eq. (1). That is, the numerator in Eq. (5) measures changes in the angle of pitch based on the pressure difference across opposing ports four and seven. The denominator nondimensionalizes the term with the probe dynamic pressure. The chief difference between Eqs. (5) and (1) is in the choice of pressures representing the probe dynamic pressure. For this flow situation it is the pressure at port four which most closely approximates the total pressure, and the average pressure of ports three and five which approximates the static pressure.

Extending this reasoning to a coefficient sensitive to changes in roll angle produces the equation

$$C_{\phi_4} = \frac{P_3 - P_5}{P_4 - (P_3 + P_5)/2} \tag{6}$$

where the numerator is proportional to changes in roll angle based on the pressure difference across ports three and five. Again, the denominator nondimensionalizes the term with the probe dynamic pressure.

Finally, the coefficient of compressibility is given by

$$C_{M_4} = \frac{P_4 - (P_3 + P_5)/2}{P_4} \tag{7}$$

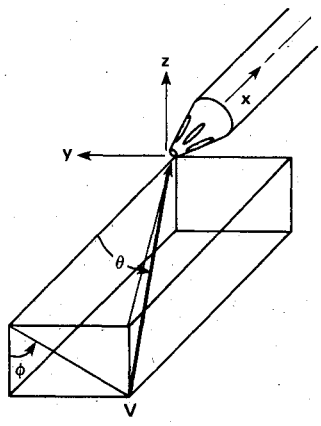

Fig. 3 High angle reference system.

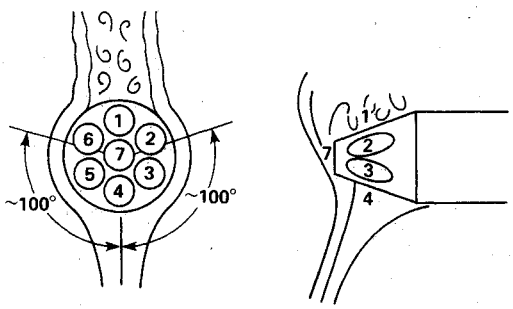

Fig. 4 Flow at high angle of attack.

This equation is analogous to Eq. (4) in that the numerator is the probe dynamic pressure and the denominator approximates the total pressure.

The subscript *4* identifies these definitions as only being valid when the flow approaches the probe within the sector centered on port four. In general form, the complete set of high angle coefficients consists of

$$C_{\theta_n} = \frac{P_n - P_7}{P_n - (P_{n-} + P_{n+})/2}, \quad C_{\phi_n} = \frac{P_{n-} - P_{n+}}{P_n - (P_{n-} + P_{n+})/2}$$

$$C_{M_n} = \frac{P_n - (P_{n-} + P_{n+})/2}{P_n} \tag{8}$$

Flow Properties

The local flow angle is represented in terms of angle of attack α_T and angle of sideslip β_T for low angle measurements, and in terms of pitch angle θ and roll angle ϕ for high angle measurements. These properties are calculated directly from their respective polynomial functions. The local total and approximate dynamic pressures, however, are not calculated directly. These two properties are represented in a dimensionless form by defining two additional pressure coefficients. These coefficients, rather than the pressures themselves, are determined from polynomial functions.

For low angles, these flow property coefficients are defined as

$$Co = \frac{P_7 - P_{o_L}}{P_7 - \bar{P}_{1\text{-}6}}, \quad Cq = \frac{P_7 - \bar{P}_{1\text{-}6}}{P_{o_L} - P_{\infty_L}} \tag{9}$$

The total pressure coefficient Co corrects for the difference between the probe's estimation of total pressure (P_7) and the actual total pressure. The difference is nondimensionalized by the probe dynamic pressure. The approximate dynamic pressure coefficient Cq accounts for the difference between the probe dynamic pressure and the approximate dynamic pressure, expressing the two as a dimensionless ratio.

These coefficients are derived for high angle flow with the same rationale used to obtain their low angle counterparts. That is, the choice of pressures used to approximate the total and probe dynamic pressures depends on the sector the flow approaches. The result is the set of equations

$$Co_n = \frac{P_n - P_{o_L}}{P_n - (P_{n-} + P_{n+})/2}, \quad Cq_n = \frac{P_n - (P_{n-} + P_{n+})/2}{P_{o_L} - P_{\infty_L}} \tag{10}$$

After the total and approximate dynamic pressure coefficients are calculated, the local total and approximate dynamic pressures are extracted from Eqs. (9) for low flow angles or Eqs. (10) for high flow angles. For example, solving Eqs. (9) for the local total and approximate dynamic pressures results in the two identities

$$P_{o_L} = P_7 - Co(P_7 - \bar{P}_{1\text{-}6}), \quad P_{o_L} - P_{\infty_L} = \frac{P_7 - \bar{P}_{1\text{-}6}}{Cq} \tag{11}$$

The local Mach number is then determined from standard isentropic gas-dynamic equations. A similar procedure is extended to Eqs. (10) for the outer sectors.

Division of Angular Space

Several sets of coefficients for various regions about the probe have been established. A means of determining which of these sets to use is now needed. The method employed is presented in Fig. 5 and defines a low angle inner sector and six high angle periphery sectors. The pressure port with the highest pressure indicates the general direction from which the oncoming velocity vector is approaching. A given data point is allocated to the sector corresponding to the port with the highest pressure. This method ensures that flow over the

adjacent ports remains attached, and that the appropriate set of equations is applied.

Determining the Calibration Constants

During probe calibration, data are taken to provide a representative sampling of all possible flow conditions. The data points are allocated to the appropriate sectors and the corresponding pressure coefficient variables are evaluated. A third-order polynomial expansion of the coefficients is used to represent the flow properties. For the inner sector this expansion takes on the form

$$A_i = (K_1^A + K_2^A C_{\alpha_T} + K_3^A C_{\beta_T} + K_4^A C_{M_7} + K_5^A C_{\alpha_T}^2 + K_6^A C_{\beta_T}^2 + K_7^A C_{M_7}^2 + K_8^A C_{\alpha_T} C_{\beta_T} + K_9^A C_{\alpha_T} C_{M_7} + K_{10}^A C_{\beta_T} C_{M_7} + K_{11}^A C_{\alpha_T}^3 + K_{12}^A C_{\beta_T}^3 + K_{13}^A C_{M_7}^3 + K_{14}^A C_{\alpha_T}^2 C_{\beta_T} + K_{15}^A C_{\alpha_T}^2 C_{M_7} + K_{16}^A C_{\beta_T}^2 C_{\alpha_T} + K_{17}^A C_{\beta_T}^2 C_{M_7} + K_{18}^A C_{M_7}^2 C_{\alpha_T} + K_{19}^A C_{M_7}^2 C_{\beta_T} + K_{20}^A C_{\alpha_T} C_{\beta_T} C_{M_7})_i \quad (12)$$

where A is one of the flow properties α_T, β_T, Co, or Cq. A sample set of m data points is taken for the given sector (a minimum of 20 samples must be taken to uniquely define the 20 K's). The subscript i identifies the equation as representing the value of the flow property measured for the ith data point. A set of four such equations, each equation representing one of the four flow properties, is determined for each of the seven probe sectors. The K's are calibration constants where the subscript identifies the term in the expansion and the superscript identifies which of the four expansions. The terms C_{α_T}, C_{β_T} and C_{M_7} are the appropriate pressure coefficient variables evaluated for the ith data point.

In the case of high angle (outer sector) measurement, Eq. (12) is modified by replacing C_{α_T}, C_{β_T}, and C_{M_7} with C_{θ_n}, C_{ϕ_n}, and C_{M_n}, respectively. The term A then represents one of the flow properties θ, ϕ, Co_n, or Cq_n.

For the inner sector, sampled with m data points, the resulting set of Eqs. (12) is represented in matrix notation as

$$\begin{bmatrix} A_1 \\ A_2 \\ A_3 \\ \cdot \\ \cdot \\ \cdot \\ A_m \end{bmatrix} = \begin{bmatrix} 1 & C_{\alpha_{T_1}} & C_{\beta_{T_1}} & C_{M_{7_1}} & \cdots & C_{\alpha_{T_1}} C_{\beta_{T_1}} C_{M_{7_1}} \\ 1 & C_{\alpha_{T_2}} & C_{\beta_{T_2}} & C_{M_{7_2}} & \cdots & C_{\alpha_{T_2}} C_{\beta_{T_2}} C_{M_{7_2}} \\ 1 & C_{\alpha_{T_3}} & C_{\beta_{T_3}} & C_{M_{7_3}} & \cdots & C_{\alpha_{T_3}} C_{\beta_{T_3}} C_{M_{7_3}} \\ \cdot & \cdot & \cdot & \cdot & & \cdot \\ \cdot & \cdot & \cdot & \cdot & & \cdot \\ \cdot & \cdot & \cdot & \cdot & & \cdot \\ 1 & C_{\alpha_{T_m}} & C_{\beta_{T_m}} & C_{M_{7_m}} & \cdots & C_{\alpha_{T_m}} C_{\beta_{T_m}} C_{M_{7_m}} \end{bmatrix} \begin{bmatrix} K_1 \\ K_2 \\ K_3 \\ \cdot \\ \cdot \\ \cdot \\ K_{20} \end{bmatrix} \quad (13)$$

Equation (13) is abbreviated as

$$[A] = [C]\ [K] \quad (14)$$

where the $m \times 1$ A matrix contains m values of one of the four flow properties, the $m \times 20$ C matrix contains the corresponding expanded pressure coefficient variables, and the 20×1 K matrix contains the calibration constants.

During calibration, the quantities within the A matrix are set by the experimenter. Moreover, the local total and static pressures at the probe are equal to their freestream values. After measuring the port pressures at these preset flow conditions, the quantities within the C matrix can be calculated. The calibration procedure, therefore, involves the calculation of the unknown calibration constants of the K matrix. The calibration constants are unique to each probe

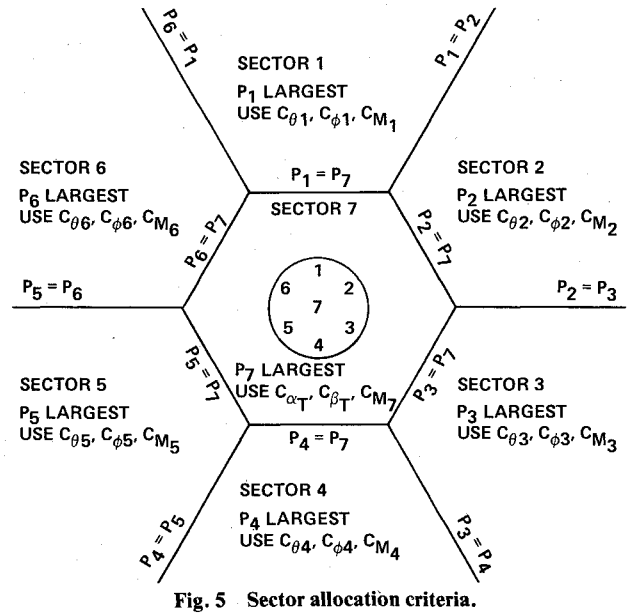

Fig. 5 Sector allocation criteria.

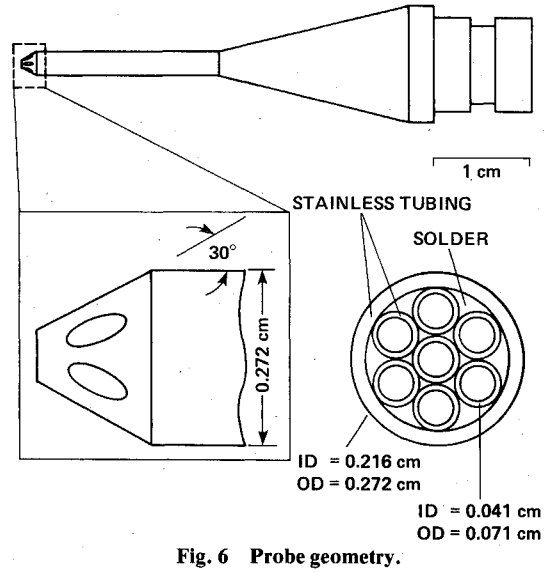

Fig. 6 Probe geometry.

and are determined with matrix algebra according to the procedure outlined by Netter and Wasserman[5]

$$[K] = [C^T C]^{-1} [C]^T [A] \quad (15)$$

Using this technique, the calibration constants are determined from a least-squares-curve fit to the experimental data.

Having determined the calibration constants, the calibration process is complete and the probe is ready for use in unknown flowfields. Once in an unknown flowfield, the highest measured probe pressure determines which set of pressure coefficients applies. These coefficients along with the calibration constants then allow the desired flow properties to be calculated explicitly from Eq. (12).

Apparatus and Procedure

Probe Geometry

The geometry of the seven-hole probe is shown in Fig. 6. The barrel has seven stainless steel tubes arranged within a larger stainless steel tube. The inner tubes pack inside the outer tube in a unique pattern that provides reasonably accurate alignment of the pressure ports. Once in place, the tubes are soldered together. The tip is then machined to form

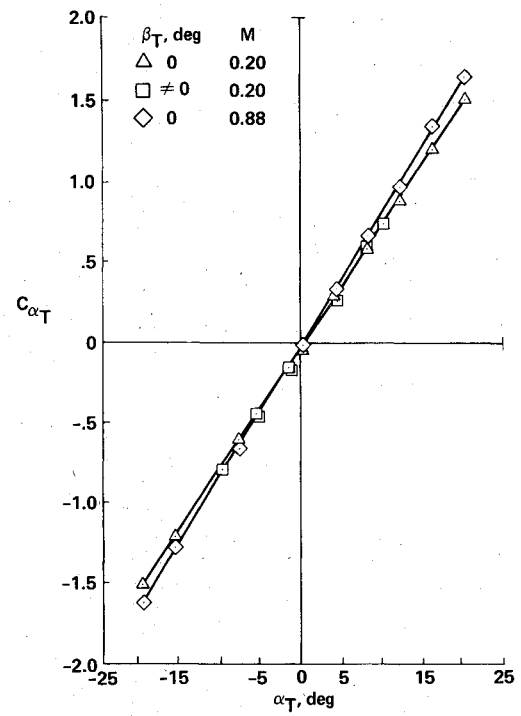

Fig. 7 Angle-of-attack coefficient vs angle of attack.

a cone with a half-angle of 30 deg. The probe barrel has a diameter of 0.272 cm and is 2.03-cm long. The diameter increases to a maximum of 1.19 cm, forming a conical afterbody with a half-angle of 15 deg.

Test Conditions

The calibration test conditions were chosen to correspond with the test conditions most commonly used for the research programs of Ref. 1. A Reynolds number of 9.84×10^6/m was used. Data were obtained at Mach numbers of 0.20, 0.39, 0.53, 0.65, 0.77, and 0.88. Limited data were also taken at Reynolds numbers of 13.12 and 14.76×10^6/m to investigate Reynolds number effects.

Angles at which data were taken were selected to provide a homogeneous sample of the data space for a given sector. To ensure that a selected point fell within the desired sector, points expected to fall on a sector boundary were avoided. The boundary between the inner and the outer sectors was expected to fall between 25 and 30 deg of pitch. Therefore, the inner sector pitch angles ranged from 0 to 24 deg in 4-deg increments. Pitch angles for the outer sectors ranged from 30 to 85 deg in 5-deg increments. The boundaries between the outer sectors were expected to fall at roll angles of 30, 90, 150, 210, 270, and 330 deg. Therefore, data were taken in 10-deg increments at a starting roll angle of 5 deg.

Pitch and roll angle sensors were calibrated prior to data acquisition to permit direct measurement of the probe pitch and roll angles. The standard errors of the angle sensor readouts were 0.20 deg in pitch and 0.55 deg in roll (95% confidence).

Results and Discussion

Four seven-hole cone probes were calibrated simultaneously in the Ames 2×2-ft transonic wind tunnel. Results for probe two are presented in the following sections. These results are typical of all four probes calibrated.

Inner Sector

Figure 7 shows the variation of the inner sector angle of attack coefficient with angle of attack. Data are plotted for probe orientations with both zero and nonzero sideslip angles at Mach 0.20 and with zero sideslip angle at Mach 0.88. The data show a linear relationship between C_{α_T} and α_T, thus supporting the selection of pressures defining C_{α_T}. Further, points with nonzero values of β_T (square symbols) correlate well with those points at orientations with zero sideslip angle. This indicates that C_{α_T} is independent of sideslip angle. Unlike sideslip angle, Mach number has a noticeable effect on C_{α_T}. The curve at Mach 0.88 is linear, as at Mach 0.20, but the slope is slightly higher. Thus, C_{α_T} is dependent on both angle of attack and, to a lesser degree, Mach number.

Similar trends are also observed for the sideslip coefficient. That is, C_{β_T} varies linearly with sideslip angle, is independent of angle of attack, and is influenced by Mach number.

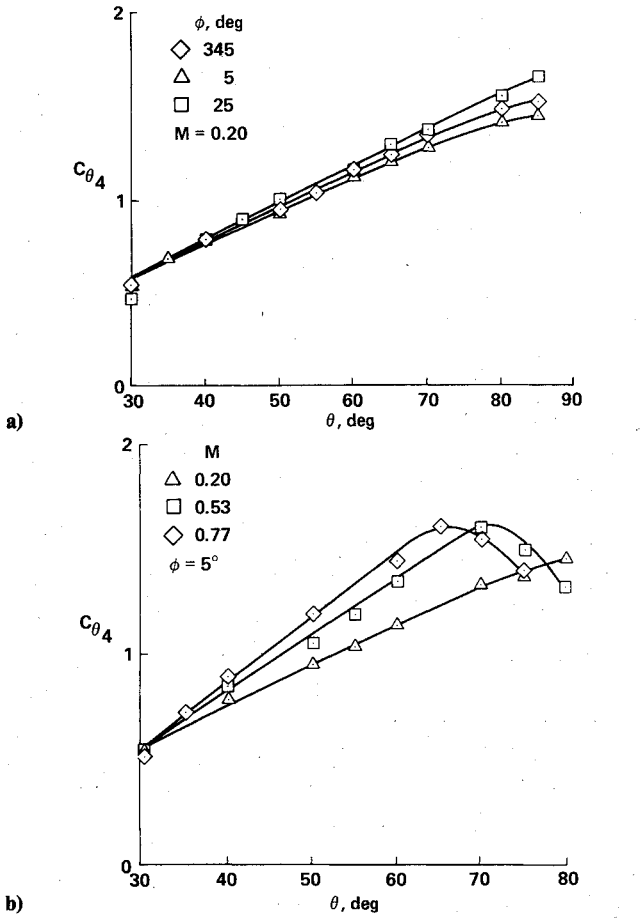

Fig. 8 Pitch coefficient vs pitch angle; a) roll angle effects, b) Mach number effects.

Outer Sectors

Figure 8 shows the variation of the pitch coefficient with pitch angle for a typical outer sector (sector four). In Fig. 8a, data are shown for three roll angles at a Mach number of 0.20. These data show that the pitch coefficient varies linearly with the pitch angle through all but very high angles. The data also show that the pitch coefficient is sensitive to roll angle.

Figure 8b shows the effect of Mach number for a roll angle of 5 deg. The plot illustrates two trends. First, the slope of the C_{θ_4} vs θ curve increases markedly with increasing Mach number. Second, the maximum angle at which flow conditions can be measured decreases with increasing Mach number. This maximum angle is defined as the point where the slope goes to zero and is believed to be caused by separation of the flow over the central port. Beyond the point of zero slope each value of C_{θ_4} corresponds to two values of θ. Since θ is a function of C_{θ_4}, flow conditions cannot be measured beyond this point. Thus, for the outer sectors, the pitch coefficient varies directly with pitch angle and is also affected by roll angle and Mach number.

Figure 9 presents plots of the roll angle coefficient (sector three) vs roll angle. The curves are well behaved and nearly

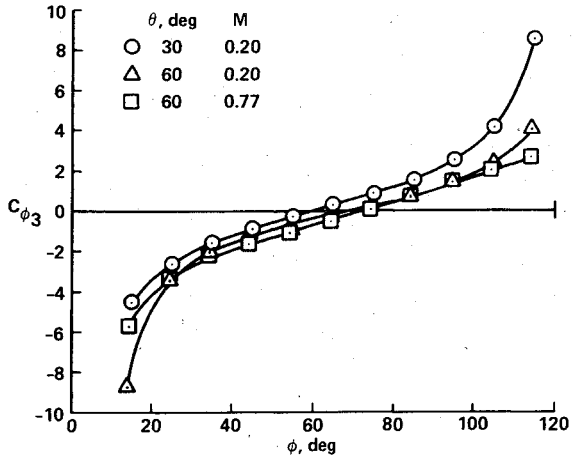

Fig. 9 Roll angle coefficient vs Mach number.

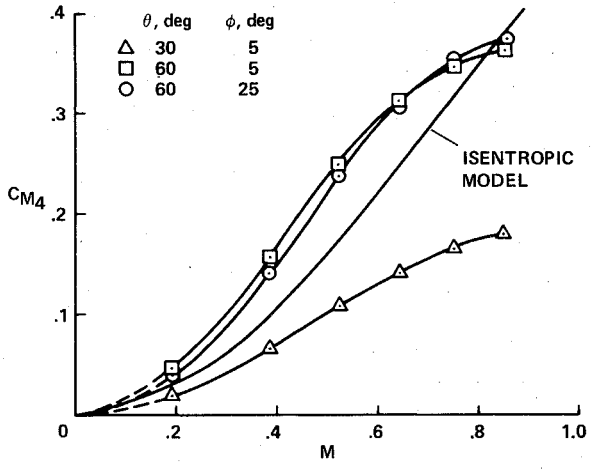

Fig. 10 Compressibility coefficient vs Mach number.

linear within the nominal sector boundaries ($\phi = 30$ and 90 deg). During calibration, variations of up to 5 deg from the nominal boundary angles were anticipated due to imperfections in the conical surface. Since the curves of Fig. 9 show no abrupt changes in slope beyond the nominal sector boundary angles, such variations do not pose any problems.

For a constant Mach number, but differing pitch angles, the roll angle coefficient is sensitive to changes in roll as well as pitch angles. At constant pitch angles, but differing Mach numbers, the curve with the higher Mach number tends to be linear over a wider range of roll angles. However, within the nominal range of the sector, the roll angle coefficient is affected less by Mach number than pitch angle.

Variation of the compressibility coefficient with Mach number is shown in Fig. 10. The relation between C_{M_4} and M is similar to the approximate dynamic to total pressure ratio vs Mach number relationship selected as the model. Discrepancies between C_{M_4} and the model are due to differences between the actual total and static pressures and those approximated by the probe. The curves at differing pitch angles (30 and 60 deg) and a single roll angle (5 deg) illustrate that the curve varies significantly with pitch angle. On the other hand, C_{M_4} is relatively unaffected by changes in roll angle. Thus, the compressibility coefficient is dependent on Mach number and pitch angle and, to a lesser extent, on changes in roll angle.

Calibration Curve Fit

The constants for the polynomial expansions were computed with a FORTRAN program based on Eq. (15). After solution of the K matrix, the data were substituted back into the polynomial expansions [Eq. (12)] to produce predicted values. These predicted values correspond to the measured values of each point of the calibration. Standard error computations were made using the difference between the predicted and measured values to determine the accuracy of the curve fit. Chauvenet's criterion[6] for data point rejection was used to remove questionable points, then the K matrix was re-evaluated. The final standard error values are given in Table 1. The effect of varying maximum total flow angle is shown in Fig. 11. Truncating data at higher pitch angles decreases the standard errors of the flow angles.

Data at the three Reynolds numbers reveal no significant influence on the results within the range of values tested. Thus, the calibration performed for the first Reynolds number is valid throughout the range of Reynolds numbers tested.

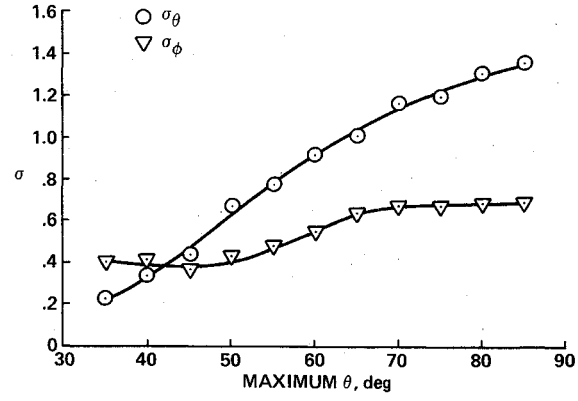

Fig. 11 Standard error vs maximum angle sampled.

Table 1 Standard errors[a]

Sector	$\sigma_\theta, \sigma_{\alpha_T}$, deg	$\sigma_\phi, \sigma_{\beta_T}$, deg	σ_{P_o/P_o}, %	$\sigma_{P_o-P_\infty/P_o-P_\infty}$, %	σ_M
1	1.05	0.64	0.3	6.8	0.030
2	1.18	0.59	0.4	5.5	0.023
3	1.27	0.68	0.4	6.3	0.026
4	1.21	0.65	0.3	5.6	0.022
5	1.12	0.72	0.3	5.3	0.021
6	1.31	0.77	0.3	5.8	0.023
7	0.25	0.22	0.1	1.8	0.007

[a] Maximum angle sampled = 75 deg.

Tunnel Stream Angularity

Stream angularity may be determined analytically from the test data. For the offset in angle of attack, C_{α_T} vs α_T for roll angles of 0 and 180 deg are plotted together. The intersection of the resulting two lines indicates the offset in angle of attack. The offset in sideslip is determined similarly, using instead C_{β_T} vs β_T for roll angles of 90 and 270 deg. Employing this technique, the angle-of-attack offsets for probes one through four were 0.62, −0.05, −0.07, and −0.36 deg, respectively. Corresponding sideslip angle offsets were approximately 0.10 deg for all four probes. These angular offsets are then taken into account prior to calibration calculations.

Summary

The theory and calibration of non-nulling seven-hole cone probes have been presented. Probe pressures are used to explicitly determine local flow properties such as flow angle, total pressure, static pressure, and Mach number. Measurement of the flow properties can be made through relatively high flow angles. The maximum flow angle at which valid measurements can be obtained varies inversely with

Mach number. The limit ranges from ~65 deg at Mach 0.88 to nearly 85 deg at Mach 0.20.

Relative flow angles, total pressure, and approximate dynamic pressures are determined from a set of polynomial functions (one set for each of seven probe sectors). The proper sector and corresponding coefficients are selected based on the highest measured port pressure. The three coefficients for angle of attack (pitch), sideslip (roll) angle, and compressibility effects effectively model their respective parameter. Each varies linearly, or nearly so, with its counterpart, all others being held constant. The use of all three coefficients as variables in the polynomial expressions is necessary to account for interdependencies evident in the data presented. These coefficients are computed from probe pressures and substituted into the polynomial functions (the constants of the functions are the result of probe calibration). With a digital computer, this series of computations is relatively simple and very fast, permitting flow properties to be obtained on a real-time basis.

Acknowledgment

The authors would like to acknowledge Lt. Col. Roger Gallington, who developed the methodology for the seven-hole cone probe.

References

[1]Nelms, W. P. and Durston, D. A., "Preliminary Aerodynamic Characteristics of Several Advanced VSTOL Fighter/Attack Aircraft Concepts," SAE Paper 801178, Los Angeles, Calif., Oct. 1980.

[2]Gallington, R. W., "Measurement of Very Large Flow Angles with Non-Nulling Seven-Hole Probes," *Aeronautics Digest—Spring/Summer 1980*, USAFA-TR-80-17, USAF Academy, 1980.

[3]Gerner, A. A. and Maurer, C. L., "Calibration of Seven-Hole Probes Suitable for High Angles in Subsonic Compressible Flows," *Aeronautics Digest—Fall/Winter 1980*, USAFA-TR-81-4, USAF Academy, 1981.

[4]Schlichting, H., *Boundary-Layer Theory*, 6th ed., McGraw-Hill, N.Y., 1968, Chap. 10.

[5]Netter, J. and Wasserman, W., "Simple Linear Regression Model in Matrix Terms," *Applied Linear Statistical Models*, Richard D. Irwin, Inc., Ill., 1975, p. 200.

[6]Holman, J. P., "Statistical Analysis of Experimental Data," *Experimental Methods for Engineers*, 3rd ed., McGraw-Hill, N.Y., 1978, pp. 65-67.